Multicomponent Vapor Sorption on Active Carbon by Combined Microgravimetry and Dynamic Sampling Mass Spectrometry

ARTICLE *in* THE JOURNAL OF PHYSICAL CHEMISTRY B · AUGUST 2002

Impact Factor: 3.3 · DOI: 10.1021/jp014625a

3 AUTHORS, INCLUDING:

Ashleigh Fletcher
University of Strathclyde
43 PUBLICATIONS **2,920** CITATIONS

SEE PROFILE

Keith Mark Thomas
Newcastle University
198 PUBLICATIONS **10,267** CITATIONS

SEE PROFILE

Multicomponent Vapor Sorption on Active Carbon by Combined Microgravimetry and Dynamic Sampling Mass Spectrometry

A. J. Fletcher,[†] M. J. Benham,[‡] and K. M. Thomas*,[†]

Northern Carbon Research Laboratories, Department of Chemistry, Bedson Building, University of Newcastle upon Tyne, Newcastle upon Tyne, NE1 7RU, United Kingdom, and Hiden Analytical Ltd., 420 Europa Boulevard, Warrington, WA5 5UN, United Kingdom

Received: December 20, 2001; In Final Form: March 25, 2002

Combined gravimetric and dynamic sampling mass spectrometry methods have been developed for the direct measurement of multicomponent vapor sorption on microporous materials. This method combines the gravimetric method for determination of the kinetics and equilibria of total adsorption, and mass spectrometry for the analysis of each adsorbate component during temperature programmed desorption. Mass spectrometry was also used for the determination of the adsorptive gas-phase concentrations during adsorption. Results are presented for adsorption of water/*n*-octane and water/*n*-butane on active carbon BAX950 using helium as the carrier gas. Marked differences were observed in the amount of water vapor adsorbed in the presence of *n*-butane compared with static water vapor and water vapor in helium. The dynamics of adsorption and desorption resulting from competitive adsorption have been investigated. The kinetics are compared with data for single component adsorption of static vapors and flowing vapors in helium. The results are discussed in terms of the diffusion processes and adsorption mechanism.

Introduction

Emissions of environmentally unfriendly species into the atmosphere are a major environmental problem and abatement methods are required to minimize these emissions. High concentrations of these species can be removed by various treatment techniques such as condensation and so forth but these methods cannot be used with very low concentrations, which are found in the final cleanup stage.[1] Activated carbons are widely used for the removal of very low (ppm) concentrations of environmentally unfriendly volatile organic compounds (VOCs) from process and air streams.[2] The adsorption process concentrates the pollutant and this may be recovered by desorption and, either recycled back to the process, or destroyed by combustion. In real situations, target species are adsorbed from complex mixtures of gases and vapors, and inevitably, competitive adsorption is involved. Competitive adsorption is also a factor in gas separation processes using pressure swing adsorption. However, very few experimental studies have been carried out and, as a result, there is very little information available on competitive adsorption.

In the case of adsorption of VOC species from ambient air, there is competitive adsorption of a pollutant with nitrogen, oxygen, and water vapor. The presence of water vapor is a very specific major problem, which varies with weather conditions and can produce degradation in the breakthrough times of other species.[3,4] Therefore, the performance of carbon adsorbent beds, for removing species from air for personal protection filters, and the abatement of emissions from process streams is inevitably influenced by multicomponent adsorption.

The primary activated carbon adsorption sites for organic species are hydrophobic sites, comprising mainly of graphene basal plane layers, and hydrophilic functional groups, where polar species, such as water, are adsorbed initially.[5−9] Clusters of water molecules develop around the functional groups with increasing relative pressure.[5] These isolated clusters of water molecules are potential barriers to diffusion of organic species.[6] At higher relative pressures either bridging occurs between these clusters or a continuous surface film is formed depending on the surface functional group distribution.[5] Pore volume filling occurs at high relative pressure but the density of the adsorbed water is usually lower than that of the liquid.[6−9] This has been ascribed to the inability of adsorbed water to form a full three-dimensional structure in microporosity.[6−9]

Competitive adsorption is difficult to study because of problems associated with quantifying the uptakes and adsorption dynamics of the various adsorbed species in multicomponent adsorption systems. The amounts adsorbed may be calculated indirectly from a complete set of adsorption isotherms for the total adsorption of the multicomponent system, using various models based on thermodynamic principles, or determined by direct measurement of the amounts of each component adsorbed.[10] In the case of the latter, there is only limited experimental information available in the literature.[11−16] Adsorption equilibrium theories for multicomponent systems have been developed based on extended Langmuir,[17] ideal adsorption solution,[18−23] and real adsorption solution[23−26] theories, but their predictive value is limited because it is not possible to select *a priori* the most suitable model without extensive experimental measurements to validate the model for the particular system of interest.[10] The experimental data required to establish and validate the model are extensive and time-consuming to obtain.

Single component isotherms can be measured by both volumetric and gravimetric methods for pure gases and vapors with the latter providing a direct measurement of the amount adsorbed.[27] Gravimetric studies of the adsorption of gases and vapors in a flow of helium have also been used.[28] Volumetric,

* To whom all correspondence should be addressed. E-mail: mark.thomas@ncl.ac.k.
[†] University of Newcastle upon Tyne.
[‡] Hiden Analytical Ltd.

10.1021/jp014625a CCC: $22.00
Published on Web 07/09/2002

gravimetric, and chromatographic methods have been used to study multicomponent isotherms, whereas breakthrough curves and flow desorption have been used, combined with the direct determination of the amounts adsorbed of each component by gas analysis to give multicomponent isotherms.[10] The adsorption kinetics are crucial for understanding gas separation processes and there is only experimental information available on pure gases and vapors in the literature.[6,7,28]

In this paper, the development of combined gravimetric and dynamic sampling mass spectrometry for the measurement of multicomponent isotherms is presented. This method provides direct measurements of the amounts of each component adsorbed and adsorption kinetics. Applications of the technique are demonstrated for *n*-butane/water and *n*-octane/water systems, which are models for the adsorption of VOCs from ambient air, where the relative humidity may change with prevailing weather conditions. The techniques also have applications in gas separation processes. The results are discussed in terms of the diffusion processes and adsorption mechanism.

Experimental Section

Materials Used. The active carbon material used was BAX950 which is a wood-based carbon obtained from the Westvaco Corporation, Virginia, US. *n*-Butane (99.9% purity) was supplied by BOC Ltd. *n*-Octane (99.9% purity) was supplied by Aldrich Chemical Co.

Instrumentation. The Intelligent Gravimetric Analyzer (IGA) is an ultrahigh vacuum system which allows isotherms and the corresponding kinetics of adsorption and desorption to be determined, for set pressure or partial pressure steps.[29] The balance and pressure control system were isothermal to ±0.01 °C to eliminate changes due to variation in the external environment. The microbalance had a long-term stability of ±1 μg with a weighing resolution of 0.2 μg. The carbon sample (100 ± 1 mg) was outgassed until constant weight, at a pressure of $<10^{-6}$ Pa at 230 °C.

Static Vapor Isotherms. The liquid used to generate the vapor was degassed fully by repeated evacuation and vapor equilibration cycles of the liquid supply side of the vapor reservoir. The vapor pressure was gradually increased, over a time-scale of ~30 s to prevent disruption of the microbalance, until the desired value was achieved. Pressure control was via the use of two transducers with ranges 0−0.2 and 0−10 kPa, each with an accuracy of 0.02% of the specified range. The pressure was maintained at the set point by active computer control of the inlet/outlet valves throughout the duration of the experiment. The mass uptake was measured as a function of time and the approach to equilibrium monitored in real time with a computer algorithm. After equilibrium was established, the vapor pressure was increased to the next set pressure value, and the subsequent uptake was measured until equilibrium was reestablished. The increase in weight due to adsorption for each pressure step was used to calculate the kinetic parameters for adsorption using an appropriate kinetic model. The errors in the calculated rate constants were obtained from fitting the data to the relevant kinetic model and are typically better than ±2%. The sample temperature was monitored throughout the experiment and the variation was minimal (<0.1 °C). The isotherms were repeatable to an accuracy of better than 1%.

Isotherms under Vapor Flow Conditions. A similar procedure was used to obtain the isotherms in flowing carrier gas conditions. The sample was weighed continuously in the presence of a helium gas flow. The vapors were introduced from a thermostated saturated vapor generator and the output of the generator was mixed with a flow of pure helium to provide a vapor stream with a specific partial pressure of vapor. The total flow rate throughout the experiments was kept constant at 500 ± 1 cm^3 min^{-1}, whereas the pressure was maintained constant at 100 ± 0.1 kPa and the temperature variation was <0.1 °C. The concentration of water vapor in the vapor stream was monitored using a capacitance polymer film type sensor and the variation due to fluctuations induced through the flow control itself was ~0.1%. The overall accuracy was tested in the case of water vapor using saturated solutions of LiCl, NaCl, and KCl of known vapor pressure for comparison with preset vapor concentrations from the vapor generator. Microgravimetry was used to detect differences in the vapor pressures of the saturated solutions and the vapor from the vapor generator. The overall accuracy of calibration was 1%, and this is limited by the accuracy of the vapor pressure of the salt solutions. The mass uptake and approach to equilibrium were monitored for each change in vapor phase concentration, in a manner similar to the static vapor isotherms.

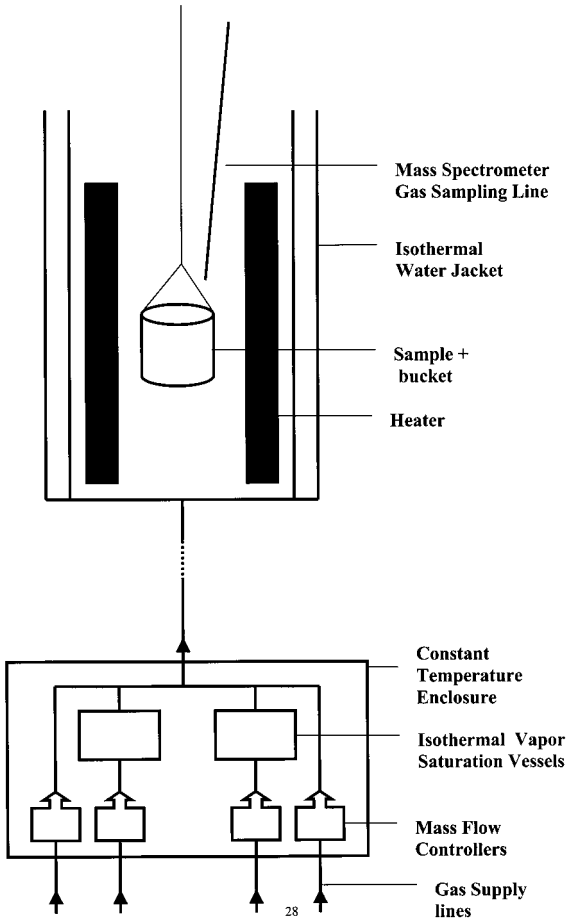

Figure 1. Schematic diagram of the combined gravimetric and dynamic sampling mass spectrometry apparatus for multicomponent adsorption studies.

Multicomponent Isotherms by Combined Microgravimetry and Dynamic Sampling Mass Spectrometry. The fully automated instrument designed for this investigation is based on the (IGA) instrument used for the studies of single component isotherms.[29] A schematic diagram of the apparatus is shown in Figure 1. The sample was weighed continuously in the presence of a carrier gas flow regulated upstream at constant total pressure in the balance chamber. The pressure was regulated to 100 ± 0.1 kPa in all the competitive adsorption experiments. The vapors were introduced from two thermostated vapor generators and fed to a reactor, housing the sample with a separate

isothermal jacket. The concentration of each component was varied by controlling the flow through the independent helium and helium + saturated vapor lines for each vapor saturation vessel. Mass flow controllers with an accuracy of ±1% were used to control the flow of each component. The total flow rate in all the experiments was 500 ± 1 cm^3 min^{-1}. The mass spectrometer signals for each species were calibrated by comparison with the known vapor concentration determined from mixing helium and saturated vapor/helium flow streams.

A Hiden HPR-20 series quadrupole mass spectrometer was used for gas analysis from the sample position via a heated capillary and direct source inlet. The adsorbed species were quantified by temperature programmed desorption and continuous gas analysis. This was achieved using an independent heating element at the sample position which was capable of controlled ramp desorption from 0.1 to 50 °C min^{-1}. The mass spectrometric analysis during temperature programmed desorption was carried out under conditions where the signal response was linear with concentration and not subject to saturation effects.

Vapor Pressure Calculations. The saturated vapor pressures were calculated using the following equation[30,31]

$$\log_{10} p = A - \frac{B}{T + C} \tag{1}$$

where p is the saturated vapor pressure (Torr), T is the temperature in degrees Celsius, and A, B, and C are constants defined by the adsorbate: water (−10 to +110 °C): A = 8.095 53, B = 1747.32, C = 235.074; n-butane (−77 to + 50 °C) A = 6.808 96, B = 935.86, C = 238.73; n-octane (10 to 152 °C), A = 6.918 68, B = 1351.99, C = 209.15.

Results and Discussion

Multicomponent Isotherm Analysis. Gravimetric measurements of competitive adsorption give the absolute total of adsorbed species. Direct analysis of the adsorbed components can be obtained using temperature programmed desorption profiles. This method is most likely to provide unequivocal results where the adsorbed species are not miscible, i.e., n-octane or n-butane and water vapor. Multicomponent adsorption can be studied in a flowing system with helium being the preferred carrier gas because of the minimal adsorption of helium at room temperature.[28] A schematic diagram of the apparatus, which combines gravimetric and dynamic sampling mass spectrometry is shown in Figure 1. In the design of the apparatus the following issues need to be considered:

(1) accurate mixing of vapor streams under precise temperature and pressure,

(2) the effect of the helium carrier gas on the adsorption characteristics of a single component,

(3) repeatability of the gravimetric system in response to the flow of multicomponent vapor streams,

(4) the response of the mass spectrometer to avoid saturation of the signal,

(5) direct measurement of gas-phase compositions during the adsorption process, and

(6) direct measurement of amounts of adsorbed species using temperature programmed desorption.

The accuracy of direct measurement of the amounts of adsorbed species is critical and this aspect is examined in this paper.

Comparison of Static Vapor and Vapor in Helium Isotherms. The multicomponent adsorption system is based on mixing streams of saturated vapor in helium, as the carrier gas, and pure helium so that the vapor pressure of each component vapor in the gas mixture is controlled. The accuracy of mixing of the two streams was established to be <1%, by comparing samples of saturated solutions of various salts of known vapor pressure with preset vapor concentrations, using microgravimetry to monitor the equilibrium.

The effect of the helium carrier gas, which is adsorbed to a very small extent, on the adsorption characteristics needs to be established, for adsorptives with widely different properties, by comparing isotherms measured under both static and flowing vapor conditions with helium as the carrier gas. This is also a test of the accuracy of setting the partial vapor pressures in the flowing system. Figures 2a and 2b show a comparison of the isotherms for static vapor and vapor/helium flow systems for water and n-octane, respectively. Water and n-octane adsorption on active carbon BAX950 have type III and type I/II isotherms in the IUPAC classification scheme, respectively. It is apparent that the adsorption isotherms of both hydrophobic and hydrophilic vapors on active carbon were not affected significantly by the presence of helium. Previous comparisons of the adsorption of oxygen and nitrogen as pure gases and in the presence of helium on a carbon molecular sieve also showed that helium did not have a significant effect on the adsorption isotherm.[28] Therefore, the use of helium as the carrier gas does not have a significant effect on the amounts of gases and vapors adsorbed on active carbons at a given relative pressure.

Linear driving force (LDF), combined barrier resistance/Fickian diffusion and Fickian models provide satisfactory descriptions, in most cases, of the adsorption kinetics of various gases/static vapors on carbon molecular sieves,[28,32,33] active carbons,[6,7,28,34−36] and porous metal organic framework materials[37] depending on the adsorptive and experimental conditions. The LDF model is described by eq 2

$$M_t/M_e = 1 - \exp(-kt) \tag{2}$$

where M_t is the mass uptake at time t, M_e is the mass uptake at equilibrium, and k is the kinetic rate constant. The adsorption kinetics can be compared in terms of the rate constant (k) for the LDF model, which can be determined from either the gradient of the $\ln(1 - M_t/M_e)$ against time plot or by fitting the adsorption uptake curves to eq 2. The adsorption kinetics follow the linear driving force model for static water (up to $p/p^0 \approx 0.97$) and n-octane (up to $p/p^0 = 0.175$) vapors and the adsorption of both vapors from helium also follow this model. A comparison of typical adsorption kinetic rate constants for water vapor and water vapor/helium, and n-octane and n-octane/helium, are shown in Figure 3a and b, respectively. The rate constants for n-octane static vapor adsorption increase with increasing relative pressure to $\sim 4 \times 10^{-2}$ s^{-1} at relative pressure $p/p^0 \approx 0.175$. In contrast, the adsorption of n-octane in helium is an order of magnitude slower ($\sim 4 \times 10^{-3}$ s^{-1} at relative pressure $p/p^0 \approx 0.175$) but also increases with increasing relative pressure and surface coverage. A comparison of the adsorption of static water vapor and water vapor in helium at 100 kPa total pressure are shown in Figure 3a. The rate constants for pressure steps above relative pressure $p/p^0 \approx 0.2$ are much slower ($< 5 \times 10^{-3}$ s^{-1}) than for adsorption of static n-octane vapor. The rate constants are similar for both static water vapor and water vapor in helium and decreased with increasing relative pressure and surface coverage.

Previous studies of the adsorption kinetics of oxygen and nitrogen as pure gases and in the presence of helium on a carbon molecular sieve, used for air separation, showed that helium decreased the adsorption kinetic rate constants for oxygen to a

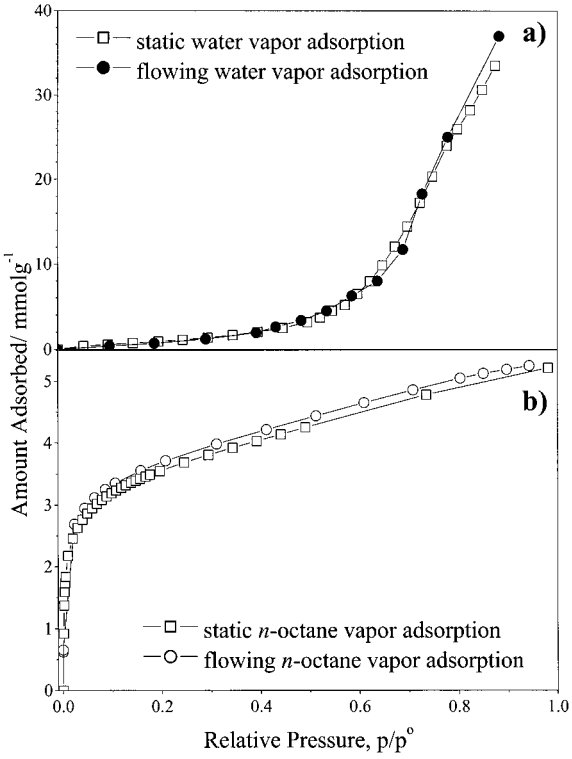

Figure 2. Comparison of adsorption isotherms for static vapor and vapor/helium (100 kPa total pressure) on active carbon BAX950 at 25 °C (a) water, (b) *n*-octane.

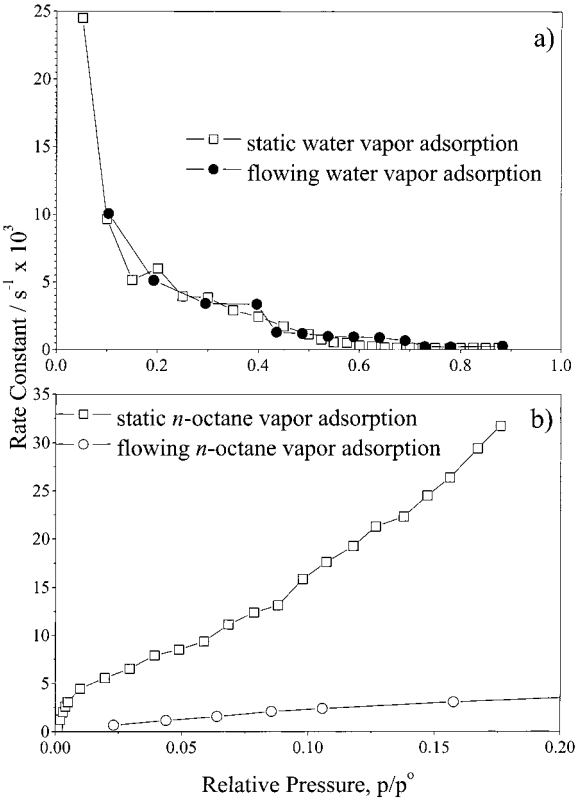

Figure 3. Comparison of adsorption kinetics for static vapor and vapor/helium (100 kPa total pressure) on active carbon BAX950 at 25 °C (a) water, (b) *n*-octane.

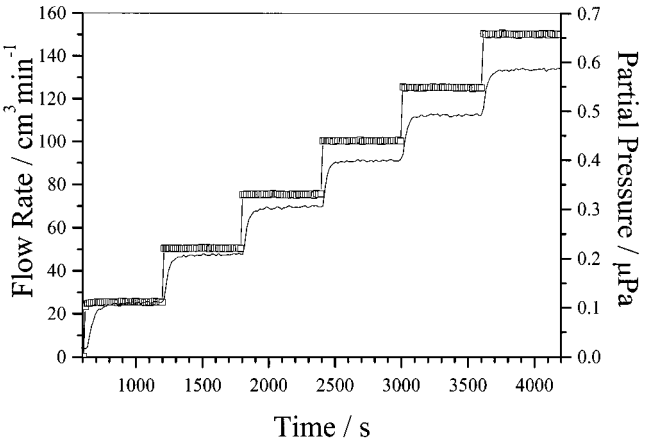

Figure 4. Mass spectrometer calibration showing the response curve of partial pressure versus partial flow rate of saturated water vapor in helium (total flow rate 150 cm^3 min^{-1}, 21 °C) versus time.

small extent (~30−37% depending on surface coverage) but had little or no effect on the adsorption of nitrogen (~5%).[28] The adsorption rate constants for nitrogen adsorption (2.1−3.3 × 10^{-4} s^{-1}) were typically a factor of ~35−40 times slower than oxygen adsorption (83−114 × 10^{-4} s^{-1}) at the same surface coverage.[28] These results are similar to those in this study showing that helium only has an effect when the adsorption kinetics are relatively fast.

Gravimetric Repeatability Studies for Multicomponent Systems. The repeatability of the gravimetric measurements for the adsorption of *n*-octane ($p/p^0 = 0.1$) after preadsorption of water vapor ($p/p^0 = 0.6$) in helium carrier gas (total pressure = 100 kPa) was investigated. The overall repeatability was excellent with a total weight uptake of 30.44 ± 0.22 wt % for 4 repeat experiments. The predominant factor in obtaining reproducibility for the adsorption measurements is the accuracy of temperature control, which is, of course, critical for all vapor phase experiments. Independent isothermal control of sample temperature to ±0.02 °C or better was required and the anti-condensation heating of enclosures was regulated within ±0.1 °C. Analysis of the uptake curves showed that they followed an LDF model. The rate constants had errors in the range 1.6−1.8% of the observed value based on analysis of over 90% of the adsorption data. The average rate constant for 4 repeat runs was 1.445 ± 0.005 × 10^{-4} s^{-1} for over 90% of the data This corresponds to an error of 0.33% of the average value for the rate constant. The standard deviations for the rate constant measurements for individual runs were <2% of the determined value. The overall rate constant and the weight uptake are a result of *n*-octane vapor adsorbed and water desorbed.

Mass Spectrometric Calibration. In the mass spectrometric analysis of the gas phase concentrations of adsorptives and desorbed species, the key issue is the linearity and calibration of the mass spectrometer. This is most difficult in the case of water vapor because of the difficulty in removing water vapor completely from mass spectrometer systems leading to the presence of background water vapor in the spectrometer, which has an effect on the accuracy of measurements. Figure 4 shows the calibration graph for the mass spectrometer signal versus the water vapor concentration expressed as the flow rate of the saturated water vapor/helium with the total flow rate of the vapor/helium and helium flow streams being 150 cm^3 min^{-1}. The mass spectrometer signal takes about 1 min to reach a plateau and this is due to mass transfer in the instrument. The calibration was very close to linearity with a regression coefficient of 0.999 77 and a gradient of 3.884 ± 0.038 × 10^{-6} mPa cm^{-3} min. This corresponds to a ratio of the partial pressure in the mass spectrometer to water vapor pressure in the vessel of 2.336 ± 0.023 × 10^{-10}.

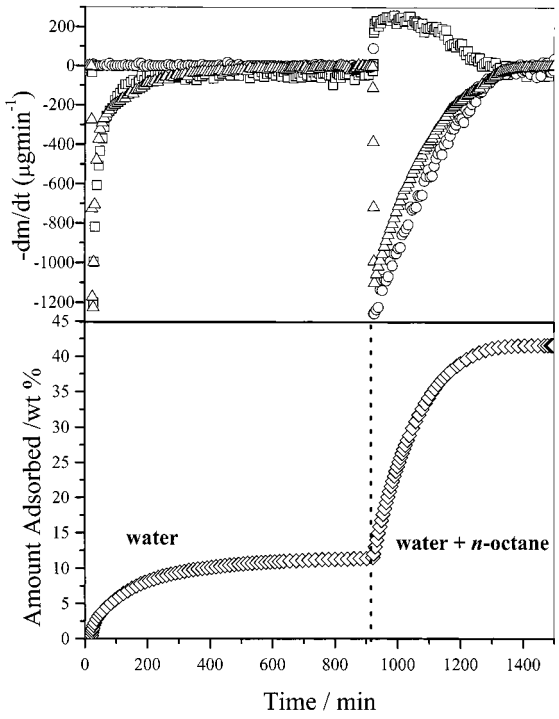

Figure 5. Mass spectrometric, gravimetric (◇) and differential gravimetric (△) adsorption 'signatures' of sequential adsorption of water (□, $p/p^0 = 0.6$) and *n*-octane (○, $p/p^0 = 0.1$) in helium (100 kPa) on active carbon BAX950 (only every 10th point included for clarity).

Comparison of Gravimetric and Mass Spectrometric Methods for Kinetic Measurements. In the case of adsorption of a single component from flowing helium, the relationship between the mass spectrometric signal curve and the gravimetric uptake curve is of fundamental importance. The gravimetric measurement provides a direct measurement of adsorption, whereas the mass spectrometer measures the adsorptive concentration very close to the sample during the adsorption or desorption process. Hence, the latter is an indirect method of following the adsorption process because it measures the influence of adsorption on the gas-phase concentration around the sample. If gas-phase diffusion is the limiting diffusion process then changes in gas-phase concentration will be observed, the mass spectrometric curve should be similar to the differential of the gravimetric uptake curve and these may be used to provide estimates of the amounts of species adsorbed and desorbed. If gas-phase diffusion has no influence on the adsorption dynamics, then the differential of the species concentration signal, obtained from the mass spectrometer signal with respect to time, should show a sharp peak with no vestigial tail when the flow stream concentration is changed for the measurement of an isotherm point, with a stable signal thereafter. This is the case when no sample is present.

Response to Perturbation in the Gas/Vapor Environment. The mass spectrometric and gravimetric adsorption signatures of sequential adsorption of water vapor ($p/p^0 = 0.6$) in helium until equilibrium was achieved followed by *n*-octane ($p/p^0 = 0.1$) adsorption in helium at a total pressure of 100 ± 0.1 kPa on active carbon BAX950 are shown in Figure 5. The mass spectrometer data are normalized to total pressure and then scaled to the equivalent mass rate to enable direct comparison with the differentiated gravimetric (DTG) measurement. In the case of isothermal equilibration, the comparison is one of mass balance. It is apparent that the water vapor adsorption up to 900 min is characterized by mass spectrometric and differential gravimetric curves of very similar shape. This observation is consistent with gas-phase molecular diffusion influencing the adsorption dynamics. The initial gravimetric water vapor uptake curve resulted in 11.42 wt % uptake and followed a combined barrier resistance/Fickian diffusion model.[38] This model is based on the existence of a barrier resistance at the surface and subsequent diffusion in a spherical microporous system by Fick's law.[39] The relevant equations for isothermal diffusion into a spherical particle with this model are as follows

$$\frac{\partial C}{\partial t} = D\left(\frac{\partial^2 C}{\partial r^2}\right) + \left(\frac{2}{r}\right)\left(\frac{\partial C}{\partial r}\right) \tag{3}$$

where D is the crystallite diffusivity (cm^2 s^{-1}), C is the sorbate concentration in the crystallite (mmol cm^{-3}), r is the radial coordinate and t is time

$$D\frac{\partial C(r_c,t)}{\partial r} = k_b\{C^*(t) - C(r,t)\} \tag{4}$$

where D is the crystallite diffusivity (cm^2 s^{-1}), k_b is the barrier resistance (cm s^{-1}), r is the radial coordinate, r_c is the radius of the crystallite (cm), t is time, C is the sorbate concentration in the crystallite (mmol cm^{-3}), and C^* is the surface concentration in equilibrium with the gas phase (mmol cm^{-3}). The parameters derived from the model are k_b the barrier resistance constant and k_d which is equal to D/r_c^2. A full description of the method used for solving the equation has been described previously.[32] The kinetic parameters for water vapor adsorption were barrier rate constant (k_b) = 2×10^{-2} cm s^{-1} and diffusion rate constant (k_d) = 6×10^{-8} s^{-1}. Similar values have been obtained for the adsorption of gases and vapors on active carbons and carbon molecular sieves.[33,34,37] However, water vapor adsorption on active carbons follow an LDF model for smaller relative pressure ($p/p^0 \approx 0.1$) increments.[6,7,28,36] When small pressure increments are used, it is apparent that the initial uptake is fast and the rate constants decrease by an order of magnitude with increasing relative pressure as cluster formation takes place around the functional groups, which leads to bridging between water molecule clusters leading to pore filling.[6,7,28,36] The change in kinetic model can be ascribed to the large change in relative pressure (0−0.6), which covers large changes in the rate constant and adsorption mechanism.

After 900 min, a flow of *n*-octane at $p/p^0 = 0.1$ was introduced as well as water vapor at $p/p^0 = 0.6$. This resulted in some water vapor desorption as shown by the positive change in the mass spectrometer signal, whereas the gravimetric curves are composites of the adsorption of *n*-octane and the desorption of water vapor. This pressure increment is considerably larger than normally used in the single component studies and this explains the difference from the LDF model observed for smaller vapor pressure increments. Integration of the areas under the mass spectra profiles indicated that only ∼2.2 wt % of the water adsorbed initially was still adsorbed after *n*-octane adsorption i.e., ∼9.22 wt % of the water adsorbed was desorbed as a result of *n*-octane adsorption. The uptake corresponding to the introduction of $0.1 \approx p/p^0$ *n*-octane resulted in a further 30.2 wt % uptake giving a total uptake of 41.62 wt %. The uptake of *n*-octane followed an LDF model with a rate constant of 1.438 ± 0.007 × 10^{-4} s^{-1} (∼90% of data used). This gravimetric measurement is a combination of *n*-octane adsorbed and water desorbed. These data are in good agreement with results presented on gravimetric repeatability presented earlier.

Figure 6 shows the sequence in Figure 5 in reverse order i.e., adsorption of *n*-octane at $p/p^0 = 0.1$ followed by water

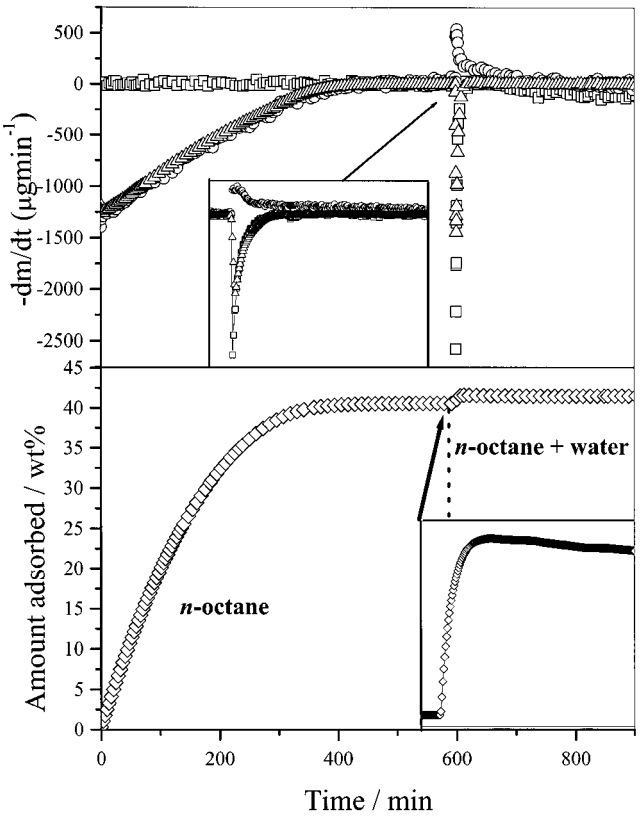

Figure 6. Mass spectrometric, gravimetric (◇) and differential gravimetric (△) adsorption "signatures" of sequential adsorption of *n*-octane (○, $p/p^0 = 0.1$) and water (□, $p/p^0 = 0.6$) in helium (100 kPa) on active carbon BAX950 (only every 10th point included for clarity). Inset figures show mass spectrometry and mass data for reduced time scale (592−660 min).

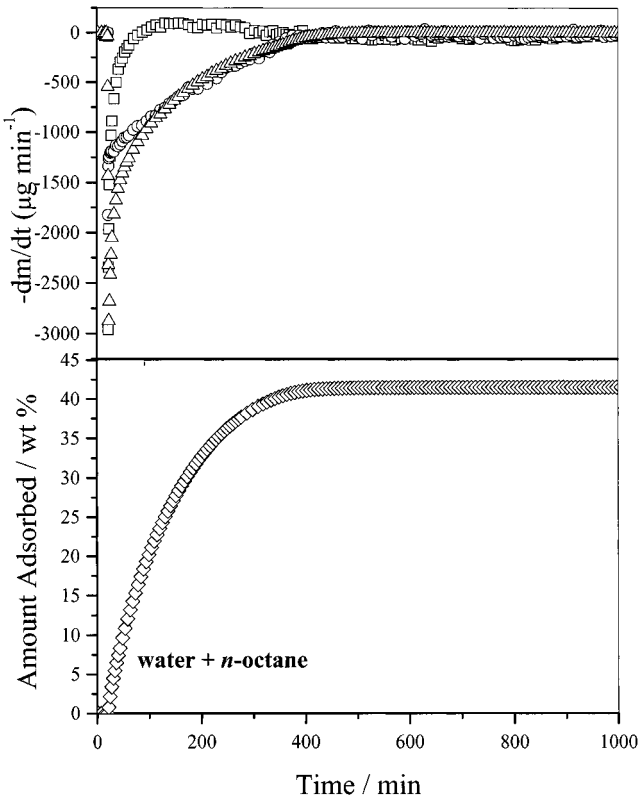

Figure 7. Mass spectrometric, gravimetric (◇) and differential gravimetric (△) adsorption "signatures" of simultaneous adsorption of *n*-octane (○, $p/p^0 = 0.1$) and water (□, $p/p^0 = 0.6$) in helium (100 kPa) on active carbon BAX950 (only every 10th point included for clarity).

vapor ($p/p^0 = 0.6$) in addition to the *n*-octane vapor after 600 min. The initial uptake of *n*-octane was 40.64 wt %. The adsorption signatures indicate that adsorption of water vapor resulted in desorption of a small amount of *n*-octane initially. Integration of the mass spectrometric profiles indicated that 3.2 wt % of water and 38.4 wt % of *n*-octane were adsorbed at equilibrium. The adsorption kinetics for both the gravimetric uptakes in the sequence followed an LDF model. The rate constants for *n*-octane adsorption and water vapor adsorption in the presence of *n*-octane were obtained from the gravimetric measurements. The gravimetric data show that the mass increases rapidly due to water vapor adsorption, which then decreases slightly before reaching a plateau. This shows the availability of the hydrophilic functional group sites and indicates that slow desorption of *n*-octane occurs. The rate constants obtained from the LDF model for *n*-octane and water vapor in the presence of *n*-octane were $1.173 \pm 0.003 \times 10^{-4}$ s^{-1} (86% of uptake data) and $5.363 \pm 0.027 \times 10^{-3}$ s^{-1} (95% of data before subsequent desorption), respectively. The overall increase in gravimetric uptake due to the adsorption of water vapor ($p/p^0 = 0.6$) after preadsorption of *n*-octane ($p/p^0 = 0.1$) was 0.95 wt % giving a total uptake of 41.59 wt %. Some desorption of *n*-octane occurred during the adsorption of water vapor.

The gravimetric and spectrometric adsorption signatures when water vapor ($p/p^0 = 0.6$) and *n*-octane ($p/p^0 = 0.1$) are adsorbed simultaneously, under conditions using helium as the carrier gas, are shown in Figure 7. The gravimetric uptake corresponded to 41.60 wt % while integration of the mass spectrometer profiles indicated that 1.7 and 39.9 wt % of water and *n*-octane vapors were adsorbed at equilibrium. These values are in good agreement with the sequence experiments in Figures 5 and 6. The initial adsorption of water vapor is much faster than *n*-octane and initially the gravimetric uptake is higher than the equilibrium value, i.e., a "super equilibrium" amount, is adsorbed and the excess is gradually desorbed as the *n*-octane is adsorbed. It is evident that the total equilibrium gravimetric uptakes for sequential and simultaneous adsorption of water ($p/p^0 = 0.6$) and *n*-octane vapor ($p/p^0 = 0.1$) were identical within experimental error and mass spectrometry studies of the gas-phase concentrations has allowed adsorption of the components to be quantified. The individual adsorption/desorption signatures can be seen in the two cases of sequential adsorption. The overall adsorption kinetics obtained from the gravimetric uptake curve followed an LDF model with a rate constant of $1.439 \pm 0.004 \times 10^{-4}$ s^{-1}. This value is slightly higher than for the adsorption of pure *n*-octane and this can be attributed to the initial faster uptake of water vapor, which is displaced subsequently as shown in the adsorption signatures in Figure 7.

The mass spectrometry studies showed rapid change in adsorptive concentrations resulting from adsorption by the active carbon and gas phase concentrations due to desorption of species in response to changes in gaseous environment resulting from adsorption on the active carbon. The former results clearly show that gas phase molecular diffusion is a factor when helium is used as the carrier gas for the vapor. When activated diffusion into the porous structure is relatively fast, gas phase molecular diffusion may be a factor in determining the overall rate of adsorption. The sequence adsorption studies demonstrate the desorption of species due to competitive adsorption. The relatively slow desorption of *n*-octane is also a limiting factor

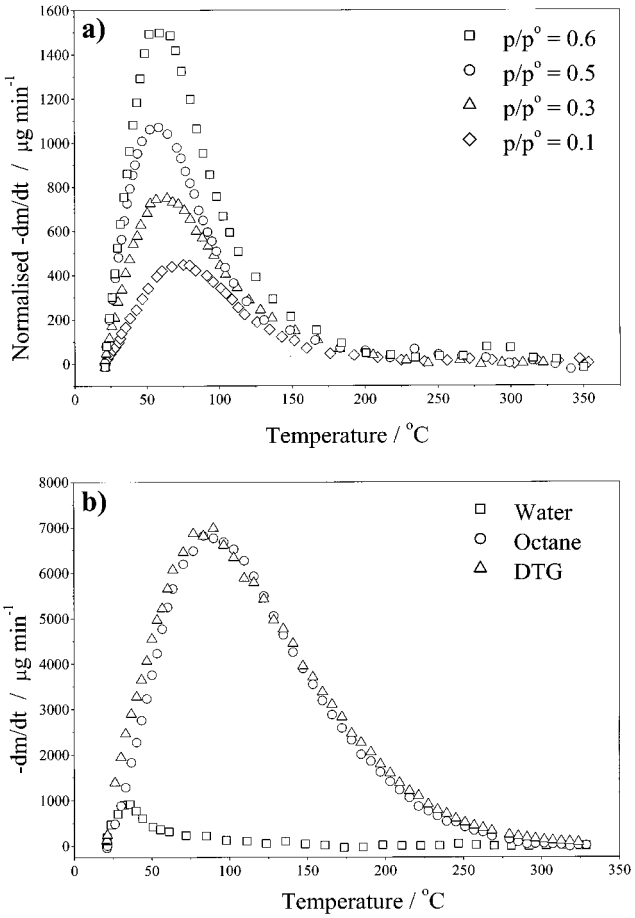

Figure 8. TPD of water from active carbon BAX950 following sequential equilibration (a) in *n*-butane ($p/p^0 = 0.023$) and water (see legend for p/p^0 details) at 21 °C (only every 10th point included for clarity); (b) in *n*-octane $p/p^0 = 0.1$ and water $p/p^0 = 0.8$ (only every 10th point included for clarity).

in the adsorption dynamics in competitive adsorption situations with water vapor.

Temperature Programmed Desorption(TPD). The amount of each adsorbed component in multicomponent isotherms can be determined directly by temperature programmed desorption of the adsorbed species coupled with spectroscopic methods in addition to micro-gravimetric analysis. The performance of the temperature programmed desorption (TPD) system was assessed. The TPD profiles of adsorbed water following sequential equilibration in *n*-butane ($p/p^0 = 0.023$) and water vapor at $p/p^0 = 0.1$, 0.3, 0.5 and 0.6 are shown in Figure 8a. The results show that the maximum in the TPD peak does not change greatly with loading. The amounts adsorbed are determined by integrating under the profiles. Figure 8b shows the differential gravimetric and mass spectrometric data for the TPD of the adsorbed vapors after the sequential loading of *n*-octane ($p/p^0 = 0.1$) and water ($p/p^0 = 0.8$). The maximum for water vapor desorption (~30 °C) is at a lower temperature than the maximum for *n*-octane desorption (~85 °C). The peak in the mass spectrometry signal is coincident with a shoulder on the DTG profile.

Competitive Adsorption Isotherms. Temperature programmed desorption profiles for water and *n*-butane and water and *n*-octane are shown in Figures 8a and b. It is apparent that these profiles are similar. The isotherm for the adsorption of water vapor in the presence of *n*-butane ($p/p^0 = 0.023$) with helium as the carrier gas was determined using these temperature

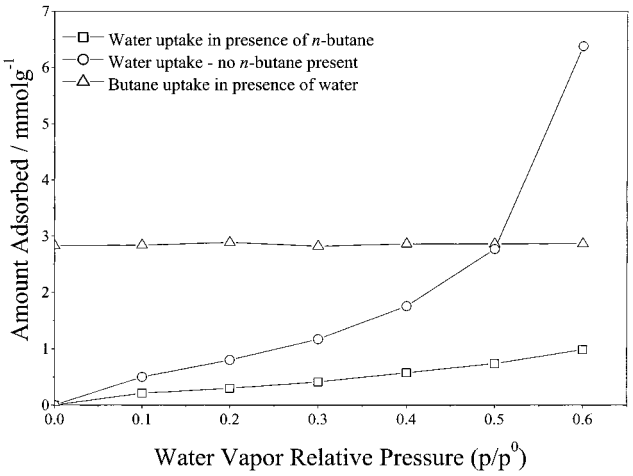

Figure 9. Adsorption isotherms of water vapor on active carbon BAX950 at 21 °C and in the presence of *n*-butane at ($p/p^0 = 0.023$) using helium as the carrier gas.

programmed desorption profiles to quantify the amount of each component adsorbed and this is shown in Figure 9. It is evident that within the limits of experimental conditions used, *n*-butane adsorption does not change significantly (within ~1%) as humidity is increased up to $p/p^0 = 0.6$ and is very similar to that for the pure gas. In contrast, the concentration of adsorbed water was, in all cases, significantly lower than the pure component isotherm and this was especially marked at high relative pressure where it is ~15% of the pure water vapor adsorption uptake. This observation is supported by the sequential adsorption studies for *n*-octane and water vapor (see Figures 5−7), where the adsorbed water in the presence of *n*-octane is ~20% that observed for static water vapor and water vapor in helium. This is clearly demonstrated by the displacement of ~80% (11.42 wt % to 2.2 wt %) of the preadsorbed water ($p/p^0 = 0.6$) by *n*-octane ($p/p^0 = 0.1$) in the sequential adsorption studies in Figure 5. The reason for this decrease in adsorbed water cannot be attributed to pore filling limitations. Active carbon BAX950 has a total pore volume of 0.83 $cm^3\ g^{-1}$, whereas 2.9 mmol g^{-1} of *n*-butane corresponds to 0.291 $cm^3\ g^{-1}$ assuming a density of 0.5788 g cm^{-3} at 20 °C[30] for the adsorbed phase, whereas 1 mmol g^{-1} of water corresponds to 0.018 $cm^3\ g^{-1}$ assuming that the density of adsorbed water = 1 g cm^{-3}. The density of adsorbed water is thought to be lower (~70−80%) than water[7−9] due to the inability of adsorbed water to form a full three-dimensional structure in microporosity but this does not affect the argument. The adsorption kinetics clearly show that equilibrium has been reached in all cases. The micropore volume obtained from extrapolation of the Dubinin−Radushkevich graph for carbon dioxide adsorption data at 0 °C was 0.18 $cm^{-3}g^{-1}$.[6]

In this system, the two adsorbates are immiscible. The water vapor is adsorbed on the hydrophilic functional groups and water molecule clusters develop around these adsorption sites, whereas *n*-butane is adsorbed on the hydrophobic graphene layers. Therefore, it is reasonable to conclude that there is no competition between the adsorbates for the same adsorption sites. The graphene layer surfaces are virtually fully covered by *n*-butane under the experimental conditions used where the amount adsorbed exceeds the micropore volume of the carbon. It is proposed that there is a strong repulsive interaction between the water molecules adsorbed in hydrophilic clusters around the oxygen functional groups and the *n*-butane adsorbed on the hydrophobic graphene layer surfaces to which the functional

groups are attached, which results in decreased water vapor adsorption. Previous studies of CH_4/H_2O adsorption on steam activated pitch-based active carbon fibers showed a noticeable enhancement of water vapor adsorption upon introduction of supercritical methane at 303 K.[40] This was attributed to transient compression of water vapor on the introduction of supercritical methane. This mechanism is not possible under the experimental conditions used in this study. Studies of the effect of moisture in microporous activated carbon on the adsorption of methane showed that the presence of adsorbed water vapor usually had a negative effect on methane adsorption for a wide range of moisture contents over the temperature range 273−298 K.[41]

Diffusion in Porous Materials. Gas-phase diffusion, Knudsen diffusion in pores and activated surface diffusion along the pore walls occur in parallel. Collisions of gas-phase molecules dominate diffusion in large pores. Knudsen diffusion becomes important when the pore dimensions are similar to the mean free path of the adsorptive. Surface diffusion, resulting from the surface concentration gradient, is the controlling process in the microporosity. The relative rates of these diffusion processes determine which is rate determining for the overall kinetic process.

Good agreement between the water and *n*-octane isotherms for adsorption of vapors in both static and flowing helium environments showed that helium had virtually no effect on the equilibrium situation. This is consistent with the very low adsorption of helium under the conditions used in the experiments. However, the presence of helium slowed the kinetics for *n*-octane adsorption markedly. Similar results were obtained for oxygen/helium adsorption on a carbon molecular sieve where the kinetics were relatively fast.[28] The adsorption signatures for commutation of water and *n*-octane vapor in helium indicate that gas-phase diffusion is influencing the adsorption kinetics. In static vapor adsorption, this limitation cannot occur provided the pressure is constant because there will not be a pressure gradient in the vapor phase. The *n*-octane isotherm is Type I/II in the IUPAC classification scheme, and the major part of the adsorption uptake occurs at low relative pressure (<100 kPa). Both gas phase and Knudsen diffusion will be dominated by the helium present, which represents over 98% of the gas phase (saturated vapor pressure (p^0) for *n*-octane and water vapor at 21 °C are 1.4764 and 2.4942 kPa, respectively). The presence of helium as the carrier gas reduces the mean free path of the molecules influencing the pore size region where Knudsen diffusion becomes significant. The collision cross-sections for helium and *n*-octane are 257 and 740.7 pm respectively but there is no generally accepted value for water molecules.[42] However, the size range 250−1000 pm represents the range of values reported for gases and vapors in the literature.[42] Therefore, the main differences in the mean free paths of molecules in static and flowing vapor adsorption studies are due to the effect of pressure. The major part of the adsorption uptake of *n*-octane occurs at pressures <1 mbar and the mean free path in static vapor is ∼70 μm compared with ∼70 nm for *n*-octane in helium at 100 kPa total pressure. Thus, the pore size where gas phase diffusion changes to Knudsen diffusion is very different. In comparison, the water vapor is type III and most of the uptake occurs at high relative pressure (>1 kPa). The mean speeds of molecules are inversely proportional to the square root of the molar mass and thus the speeds of water and *n*-octane molecules differ by a factor of ∼2.5. These factors influence the adsorption dynamics with the difference in the mean free path, resulting from the difference in total pressure under static and flowing vapor conditions, being the major factor influencing diffusion in the gas phase and in the pores. It is apparent from the adsorption signatures in the flowing system that gas-phase diffusion is a limiting factor in the cases of both *n*-octane and water vapor. The rate constants for water adsorption are slower but the vapor relative pressure increment (0−0.6) includes the initial fast rates for $p/p^0 < 0.2$, which gives rise to the gas-phase diffusion limitations. The *n*-octane adsorption kinetics in flowing helium (100 kPa total pressure) still follow the LDF model closely as observed for static vapor. The rate constants increase with increasing relative pressure but are much slower than for static vapor. However, these rate constants do not have the same meaning as when the rate-determining step is diffusion through barriers in the porous structure, as in the case of static vapor adsorption in the porous structure. In the case of water vapor, the rate constants decrease with increasing relative pressure. Therefore, at low relative pressure where the rate constants are fast, there are limitations due to gas phase diffusion. The rate constants in static vapor and flowing helium are virtually identical above $p/p^0 > 0.2$ and this is attributed to rate determining diffusion into the porous structure.

Conclusions

The development of combined gravimetric and dynamic sampling mass spectrometry for multicomponent vapor sorption is presented. Comparisons of adsorption of static and flowing vapors in helium as a carrier gas showed that the presence of helium had little or no effect on the adsorption isotherms but, in some circumstances, there was a significant effect on the adsorption kinetics. Mass spectrometric measurements of adsorption and desorption signatures showed that the kinetic effect can be attributed to changes in the gas-phase diffusion processes for adsorptives under static vapor atmosphere and flowing conditions at a total pressure of 100 kPa, which are due to differences in the mean free path of the adsorptive molecules.

Temperature programmed desorption was used to determine the amounts of both components adsorbed for the *n*-butane/water system. The studies show, within the limits of operating conditions used thus far, an invariance of *n*-butane adsorption (within ∼1%) as water relative pressure increased up to 0.6. Moreover, the amount of adsorbed water was in all cases significantly lower than the pure component isotherm. The conditions used are well below the situation where pore filling may be a limiting factor for adsorption capacity. Commutation of isothermal loading of water and *n*-octane vapor showed that displacement of preadsorbed species and changes in adsorption kinetics. The displacement of adsorbed water indicates that, even though the adsorbates are not miscible, there is a strong interaction between the hydrophobic hydrocarbon adsorbed on the graphene layers and the water molecules adsorbed in clusters around the oxygen functional groups attached to the graphene layers, which produces lower water vapor adsorption.

References and Notes

(1) Hassoun, S.; Pilling, M. J.; Bartle, K. D. *J. Environ. Monitoring* **1999**, *1*, 453.

(2) *Volatile Organic Compounds in the Atmosphere*; Hester, R. E., Harrison, R. M., Eds.; The Royal Society of Chemistry: Cambridge, 1995.

(3) Nelson, G. O.; Correia, A. N.; Harder, C. A. *Am. Ind. Hyg. Assoc. J.* **1976**, *37*, 280.

(4) Okazaki, M.; Tamon, H.; Toei, J. *J. Chem. Eng. Jpn.* **1978**, *11*, 209.

(5) Muller, E. A.; Rull, L. F.; Vega, L. F.; Gubbins, K. E. *J. Phys. Chem.* **1996**, *100*, 1189.

(6) Harding, A. W.; Foley, N. J.; Norman, P. R.; Francis, D. C.; Thomas, K. M. *Langmuir* **1998**, *14*, 3858.

(7) Foley, N. J.; Thomas, K. M.; Forshaw, P. L.; Stanton, D.; Norman, P. R. *Langmuir* **1997**, *13*, 2083.

(8) McDermot, H. L.; Arnell, J. C. *Can. J. Chem* **1952**, *30*, 177.
(9) Freeman, J. J.; Tomlinson, J. B.; Sing, K. S. W.; Theocharis, C. R. *Carbon* **1993**, *31*, 865.
(10) Malara, C.; Mencarelli, T.; Pierini, G.; Ricapito, I.; Toci, F. *Separation Technology* **1994**, 413.
(11) Sarraf, R.; Faucompre, B.; Douillard, J. M.; Partyka, S. *Langmuir* **1997**, *13*, 1274.
(12) Finger, G.; Noack, U.; Buelow, M. *Z. Phys. Chem. (Leipzig)* **1983**, *264*, 170.
(13) Keller, J. U.; Standt, R.; Tomalla, M. *Ber. Bunsen-Ges. Phys. Chem.* **1992**, *96*, 28.
(14) Bering, B. P.; Serpinskii, V. V. *Dokl. Akad. Nauk. SSSR* **1953**, *90*, 811.
(15) Dubinin, M. M.; Zaverina, E. D. *Z. Fiz. Khim. SSSR* **1949**, *23*, 469.
(16) Bering, B. P.; Serpinskii, V. V. *Z. Fiz. Khim.* **1952**, *26*, 253.
(17) Markham, E. D.; Benton, A. F. *J. Am. Chem. Soc.* **1931**, *53*, 497.
(18) Van Ness, H. C. *Ind. Eng. Chem. Fundam.* **1969**, *8*, 464.
(19) Sircar, S.; Myers, A. L. *Chem. Eng. Sci.* **1973**, *28*, 489.
(20) Richter, E.; Schutz, W.; Myers, A. L. *Chem. Eng. Sci.* **1989**, *44*, 1609.
(21) O'Brien, J. A.; Myers, A. L. *J. Chem. Soc., Faraday Trans* **1984**, *80*, 1467.
(22) O'Brien, J. A.; Myers, A. L. *Ind. Chem. Eng. Res.* **1988**, *27*, 2085.
(23) Le Van, M. D.; Vermeulen, T. *J. Phys. Chem.* **1981**, *85*, 3247.
(24) Chen, Y. D.; Ritter, J. A.; Yang, R. T. *Chem. Eng. Sci.* **1990**, *45*, 2877.
(25) Karavias, F.; Myers, A. L. *Chem. Eng. Sci.* **1992**, *47*, 1441.
(26) Dunne, J.; Myers, A. L. *Chem. Eng. Sci.* **1994**, *49*, 2941.
(27) Rouquerol, F.; Rouquerol, J.; Sing, K. *Adsorption by Powders and Porous Solids*; Academic Press: London, 1999.
(28) O'koye, I. P.; Benham, M.; Thomas, K. M. *Langmuir* **1997**, *13*, 4054.
(29) Benham, M. J.; Ross, D. K. *Z. Phys. Chem.* **1989**, *163*, 25.
(30) *Lange's Handbook of Chemistry*, 15th ed.; Dean, J. A., Ed.; McGraw-Hill: New York, 1999.
(31) *CRC Handbook of Chemistry and Physics*, 74th ed.; CRC Press: Boca Ratan, FL, 1993.
(32) Reid, C. R.; O'koye, I. P.; Thomas, K. M. *Langmuir* **1998**, *14*, 2415.
(33) Reid, C. R.; Thomas, K. M. *Langmuir* **1999**, *15*, 3206.
(34) Fletcher, A. J.; Thomas, K. M. *Langmuir* **1999**, *15*, 6908.
(35) Reid, C. R.; Thomas, K. M. *J. Phys. Chem. B* **2001**, *105*, 10 619.
(36) Fletcher, A. J.; Thomas, K. M. *Langmuir* **2000**, *16*, 6253.
(37) Fletcher, A. J.; Cussen, E. J.; Prior, T. J.; Rosseinsky, M. J.; Kepert, C. J.; Thomas, K. M. *J. Am. Chem. Soc.* **2001**, *123*, 10 001.
(38) Loughlin, K. F.; Hassan, M. M.; Fatehi, A. I.; Zahur, M. *Gas Sep. Purif.* **1993**, *7*, 264.
(39) Crank, J. *The Mathematics of Diffusion*, 2nd ed.; Clarendon Press: Oxford, 1975.
(40) Miyawaki, J.; Kanda, T.; Kaneko, K. *Langmuir* **2001**, *17*, 664.
(41) Zhou, L.; Li, M.; Sun, Y.; Zhou, Y *Carbon* **2001**, *39*, 773.
(42) Hirschfelder, J. O.; Curtiss, C. F.; Bird, R. B. *Molecular Theory of Gases and Liquids*; Wiley: London, 1964.